

Improvement of thermoelectric performances of $\text{Bi}_2\text{Sr}_2\text{Co}_{1.8}\text{O}_x$ textured materials by Pb addition using a polymer solution method

M. A. Madre¹, M. A. Torres², Sh. Rasekh¹, J. C. Diez¹, A. Sotelo^{1*}

¹ICMA (CSIC-Universidad de Zaragoza), C/María de Luna 3, 50018-Zaragoza (Spain).

² Universidad de Zaragoza, Dpto. de Ingeniería de Diseño y Fabricación, C/María de Luna 3, 50018-Zaragoza (Spain).

Abstract

$\text{Bi}_{1.6}\text{Pb}_{0.4}\text{Sr}_2\text{Co}_{1.8}\text{O}_x$ ceramics have been prepared through a polymer solution method using polyethyleneimine. From these powders, bulk textured materials have been prepared using a melt growth technique. Microstructure has been observed by scanning electronic microscopy (SEM) which has shown that samples are mainly composed by the thermoelectric phase, with small amounts of secondary phases. Electrical resistivity measurements showed very small values nearly constant with temperature, while thermopower increases from room temperature to 650°C. Power factor at 50°C is about 0.15mW/K².m and 0.30 at 650°C, which makes these ceramics good candidates for power generation applications.

Keywords: Texturing; Ceramics; Crystal growth; Electrical properties; Thermopower.

Corresponding author: A. Sotelo. ICMA (CSIC-Universidad de Zaragoza), M^a de Luna, 3. 50018 Zaragoza, Spain. Tel.: +34 976762617. Fax: +34 976761957. e-mail address: asotelo@unizar.es

1. Introduction

Since their discovery, cobaltite ceramics have attracted much attention due to their remarkable thermoelectric performances [1,2]. Many works have been published in this field searching for the obtention of bulk thermoelectric performances close to those obtained for single crystals [3]. Some of them have been devoted to produce preferential grain alignment, as templated grain growth (TGG) [4] or reactive templated grain growth (RTGG) [5], hot pressing (HP) [6], spark plasma sintering [7] and directional solidification [8]. Other studies have explored the possibility to improve thermoelectric properties of these ceramics by applying different synthesis methods which have shown to produce a remarkable influence on the final products quality and performances [9,10]. On the other hand, it has been demonstrated that small changes on the initial composition can raise their thermoelectrical performances. This modification can be realized by cation substitution, for example Gd^{+3} and Y^{+3} for Ca^{+2} in Ca-Co-O [11] or Pb^{+2} for Bi^{+3} in Bi-Sr-Co-O [3,12].

In this contribution it is presented the improvement of thermoelectric characteristics of Bi-Sr-Co-O ceramics using, at the same time, these three different modifications of polycrystalline ceramics: solution synthesis, doping and texturing techniques to produce high performance bulk thermoelectric ceramics.

2. Experimental

Synthesis of $Bi_{1.6}Pb_{0.4}Sr_2Co_{1.8}O_x$ precursors were made in several steps, as described elsewhere [9]. Adequate amounts of metallic acetates (analytical grade) were dissolved in a mixture of glacial acetic acid and distilled water (~ 40:60vol.%, respectively). Polyethyleneimine (PEI, 50wt.% water) was added (~ 1 mol PEI:2 moles $Bi_{1.6}Pb_{0.4}Sr_2Co_{1.8}O_x$) to the above solution which turned darker immediately clear indication of the cation-nitrogen coordination. Solvent evaporation was produced in a rotary evaporator reducing the initial volume to about 20%. Total solvent evaporation is performed on a hot plate at about 50°C until a dark pink thermoplastic paste is obtained. Further heating turned this paste to violet colour, followed by a partial decomposition and, finally, producing a self propagated combustion at about 300-350°C which raises immediately the temperature inside the crucible to about 750°C measured with an IR optical pyrometer.

The obtained powders were manually milled, thermally treated at 750 and 810°C for 6 hours, with an intermediate milling, and isostatically pressed at 200MPa in form of cylinders (~ 3 mm diameter and 100 mm long) which were used as feed in a laser induced melt grown system described elsewhere [13]. Growth process was performed at 30 mm/h with a relative rotation between feed and seed of 18 rpm.

As-grown materials were characterized by powder X-ray diffraction (XRD, Rigaku D/max-B). The platelet thickness was estimated from X-ray line broadening measurements according to Scherrer's formula [14]. Microstructure was studied by scanning electron microscopy (SEM, JEOL 6000) provided with an energy dispersive spectroscopy (EDS) system.

Electrical resistivity (ρ) and thermopower (S), were simultaneously determined in a LSR-3 measurement system (Linseis GmbH) between 50 and 650°C. Power factor ($PF=S^2/\rho$) has been calculated in order to determine the samples performances.

3. Results and discussion

Fig. 1 shows the XRD plot for the $\text{Bi}_{1.6}\text{Pb}_{0.4}\text{Sr}_2\text{Co}_{1.8}\text{O}_x$ samples. Most of the peaks correspond to the thermoelectric phase, with minor peaks associated to non-thermoelectrical secondary phases. The highest peaks (marked with a *) belong to the misfit cobaltite phase and are in agreement with previously reported data [3, 12, 15]. The other peaks correspond to the minor $\text{Bi}_{0.75}\text{Sr}_{0.25}\text{O}_y$ phase, with rhombohedral $\overline{R3m}(\#166)$ space group (marked with a ●) [16]. The XRD results indicate that $\text{Bi}_{1.6}\text{Pb}_{0.4}\text{Sr}_2\text{Co}_{1.8}\text{O}_x$ phase was obtained as major one with this process.

Typical fractured section of the as grown materials is presented in Fig.2a. It is clear that samples are composed of plate-like grains well stacked each other along the ab planes, most of them exceeding 100 μm in the a and b directions. On the other hand, their thickness is difficult to be measured as they are, in turn, formed by many thin individual grains. In order to overcome this problem, the individual plate-like grain thickness has been estimated from the X-ray line broadening measurements using the (0 0 2l) diffraction peaks of the $\text{Bi}_{1.6}\text{Pb}_{0.4}\text{Sr}_2\text{Co}_{1.8}\text{O}_x$ phase, according to the Scherrer's formula. The obtained mean value for the grain thickness is about 120nm which

clearly indicates that the crystal preferential growth is produced along the ab plain (the conducting CoO planes).

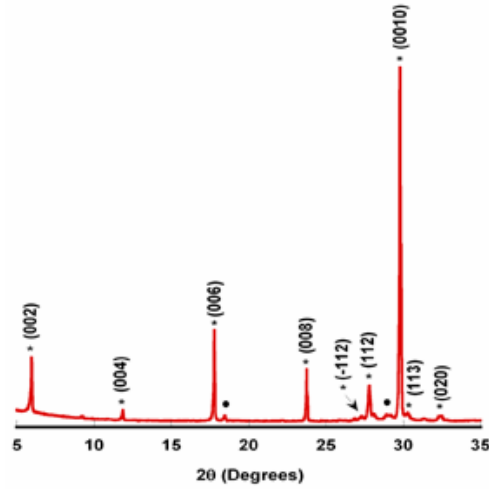


Fig. 1. XRD plot of the $\text{Bi}_{1.6}\text{Pb}_{0.4}\text{Sr}_2\text{Co}_{1.8}\text{O}_x$ samples. Peaks are marked with a * for the thermoelectric $\text{Bi}_{1.6}\text{Pb}_{0.4}\text{Sr}_2\text{Co}_{1.8}\text{O}_x$ phase; and • $\text{Bi}_{0.75}\text{Sr}_{0.25}\text{O}_y$ non thermoelectric phase ($\bar{R}3m$).

When observing the longitudinal polished section of nominal composition $\text{Bi}_{1.6}\text{Pb}_{0.4}\text{Sr}_2\text{Co}_{1.8}\text{O}_x$ (Fig. 2b) it is found that major phase is the grey one with very small amounts of secondary phases (white and dark grey contrasts). EDS analysis performed all along the samples showed that the grey contrast corresponds to the thermoelectric $\text{Bi}_{1.7}\text{Pb}_{0.4}\text{Sr}_2\text{Co}_{1.8}\text{O}_x$ phase (slightly higher Bi content than the nominal composition), white to $\text{Bi}_{0.75}\text{Sr}_{0.25}\text{O}_y$ (determined by XRD), and a new phase, seen as dark grey contrast, identified as $\text{Sr}_4\text{Co}_5\text{O}_z$. The amount of the different phases has been performed on several micrographs using Digital Micrograph software. The determined phase amounts have been around 89vol.% thermoelectric $\text{Bi}_{1.7}\text{Pb}_{0.4}\text{Sr}_2\text{Co}_{1.8}\text{O}_x$ phase, 10vol% for the $\text{Bi}_{0.75}\text{Sr}_{0.25}\text{O}_y$ and, approximately, 1vol.% $\text{Sr}_4\text{Co}_5\text{O}_z$. These data agree with the previously discussed XRD data where the $\text{Sr}_4\text{Co}_5\text{O}_z$ phase has not been detected due to its low proportion.

The temperature dependence of the resistivity is shown in Fig. 3. $\rho(T)$ curve shows a very small variation (about $\pm 4\%$ from room temperature value) with temperature, with a semiconducting-like behaviour from 50 to 300°C, changing to metallic-like behaviour from 300 to 650°C. The low resistivity values in these samples (around 14 mΩ.cm at room temperature) are due to the good

grains connectivity and small secondary phases content. Consequently, they are close to those obtained on Pb-doped single crystals ($\sim 9\text{m}\Omega\cdot\text{cm}$ at room temperature) [3], and to the values obtained for Pb-free textured materials ($\sim 15\text{m}\Omega\cdot\text{cm}$ at 275°C) [5]. Moreover, they show slightly lower resistivities than the obtained on Pb-doped samples prepared by the classical solid state method and textured using the laser growth technique ($\sim 17\text{m}\Omega\cdot\text{cm}$ at room temperature) [12], due to the higher homogeneity of the precursors obtained by solution synthesis.

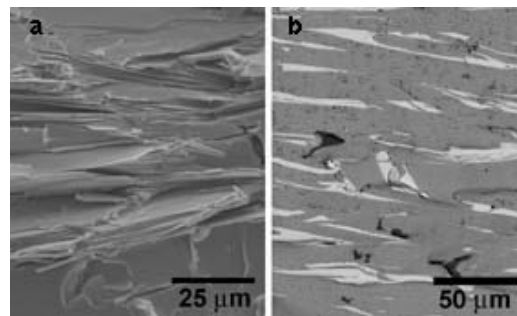


Fig. 2. Representative SEM micrographs of nominal composition $\text{Bi}_{1.6}\text{Pb}_{0.4}\text{Sr}_2\text{Co}_{1.8}\text{O}_x$ textured ceramics. a) fractured surface, and b) longitudinal polished surface. Different contrasts correspond to $\text{Bi}_{1.7}\text{Pb}_{0.4}\text{Sr}_2\text{Co}_{1.8}\text{O}_x$ (grey), $\text{Bi}_{0.75}\text{Sr}_{0.25}\text{O}_y$ (white), and $\text{Sr}_4\text{Co}_5\text{O}_z$ (dark grey).

As it can be also seen in Fig. 3, where S vs. T is represented, the values are positive in the entire temperature range, indicating a predominant hole conduction mechanism. On the other hand, they increase almost linearly from room temperature to 450°C , remaining practically constant at higher temperatures. The S values are about $145\mu\text{V}/\text{K}$ at room temperature which are higher than those obtained for textured materials ($125\mu\text{V}/\text{K}$ at 275°C) [5] or single crystals ($120\mu\text{V}/\text{K}$ at 25°C) [3]. Furthermore, it is also higher than the obtained for laser grown materials prepared from classical solid state obtained precursors ($120\mu\text{V}/\text{K}$ at 50°C) [12]. This high value is due to the reduction of the cobalt oxidation state in the CoO_2 layer, calculated from Koshibae's relation [17]. These values are about 3.50 for the measured samples (instead 3.63 for the stoichiometric ones [18]), clearly indicating that the use of the polymer solution method followed by the laser growth method generates higher amount of oxygen vacancies than the produced by another techniques.

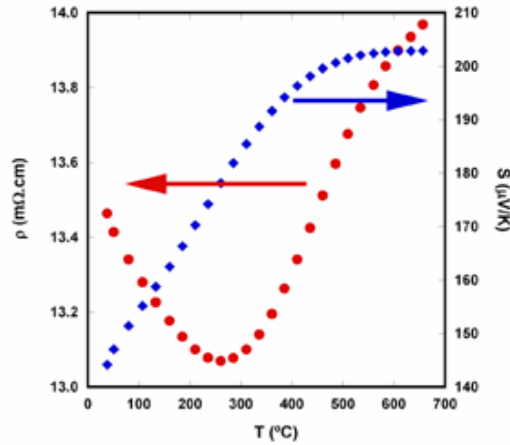


Fig. 3. Temperature dependence of ρ (•) and S (♦) for textured $\text{Bi}_{1.6}\text{Pb}_{0.4}\text{Sr}_2\text{Co}_{1.8}\text{O}_x$ materials.

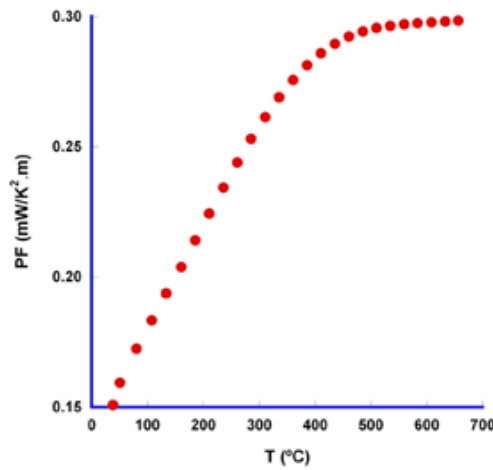


Fig. 4. Temperature dependence of PF for textured $\text{Bi}_{1.6}\text{Pb}_{0.4}\text{Sr}_2\text{Co}_{1.8}\text{O}_x$ materials.

In order to estimate the samples performances, PF values were calculated as a function of temperature and represented in Fig. 4. Comparing the graphics from S (Fig. 3) and PF (Fig. 4), they follow a very similar evolution with temperature due to the small variations of ρ with temperature in the measured range. At room temperature, the PF value of about $0.15\text{mW/K}^2.\text{m}$ is close to the obtained for single crystals ($0.16\text{mW/K}^2.\text{m}$) [3] and higher than for textured materials ($0.10\text{mW/K}^2.\text{m}$) [5,12].

4. Conclusions

Directional growth induced by laser radiation, using homogeneous precursors prepared by a polymer solution method and adequate Pb-doping, produces highly textured materials with

improved thermoelectric properties, close to the obtained in single crystals and higher than usual for textured materials.

5. Acknowledgements

This research has been supported by the Spanish Ministry of Science and Innovation-FEDER (Project MAT2008-00429) and by the Gobierno de Aragón (Consolidated Research Groups T12 and T87).

6. References

- [1] Funahashi R, Matsubara I, Ikuta H, Takeuchi T, Mizutani U, Sodeoka S. *Jpn. J. Appl. Phys.* 2000;39:L1127.
- [2] Masset AC, Michel C, Maignan A, Hervieu M, Toulemonde O, Studer F, *et al.* *J. Phys. Rev. B* 2000;62:166.
- [3] Itoh T, Terasaki I. *Jpn. J. Appl. Phys.* 2000;39:6658.
- [4] Masuda Y, Nagahama D, Itahara H, Tani T, Seo WS, Koumoto K. *J. Mater. Chem.* 2003;13:1094.
- [5] Itahara H, Xia C, Sugiyama J, Tani T. *J. Mater. Chem.* 2004;14:61.
- [6] Nan J, Wu J, Deng Y, Nan C-W. *Solid State Commun.* 2002;124:243.
- [7] Zhang FP, Lu QM, Zhang JX. *J. Alloys Compd.* 2009;484:550.
- [8] Diez JC, Rasekh Sh, Madre MA, Guilmeau E, Marinell S, Sotelo A. *J. Electronic Mater.* 2010;39:1601.
- [9] Madre MA, Rasekh Sh, Diez JC, Sotelo A. *Mater. Lett.* 2010;64:2566.
- [10] Rasekh Sh, Madre MA, Sotelo A, Guilmeau E, Marinell S, Diez JC. *Bol. Soc. Esp. Ceram. V.* 2010;49:89.
- [11] Liu HQ, Zhao XB, Zhu TJ, Song Y, Wang FP. *Current Appl. Phys.* 2009;9:409.
- [12] Sotelo A, Rasekh Sh, Guilmeau E, Madre MA, Marinell S, Diez JC. *Mater. Res. Bull.* 2011;46:2537.

- [13] Sotelo A, Guilmeau E, Madre MA, Marinel S, Diez JC, Prevel M. J. Eur. Ceram. Soc. 2007;27:3697.
- [14] Patterson AL. Phys Rev 1939;56:978.
- [15] Kato M, Goto Y, Umehara K, Hirota K, Yoshimura K. Physica B 2006;378-380:1062.
- [16] Mercurio D, Champarnaud-Mesjard JC, Frit B, Conflant P, Boivin JC, Vogt T. J. Solid State Chem. 1994;112:1.
- [17] Koshibae W, Tsutsui K, Maekawa S. Phys. Rev. B 2000;62:6869.
- [18] Maignan A, Pelloquin D, Hebert S, Klein Y, Hervieu M. Bol. Soc. Esp. Ceram. V. 2006;45:122.

Figure captions

Fig. 1. XRD plot of the $\text{Bi}_{1.6}\text{Pb}_{0.4}\text{Sr}_2\text{Co}_{1.8}\text{O}_x$ samples. Peaks are marked with a * for the thermoelectric $\text{Bi}_{1.6}\text{Pb}_{0.4}\text{Sr}_2\text{Co}_{1.8}\text{O}_x$ phase; and \bullet $\text{Bi}_{0.75}\text{Sr}_{0.25}\text{O}_y$ non thermoelectric phase ($\bar{R}3m$).

Fig. 2. Representative SEM micrographs of nominal composition $\text{Bi}_{1.6}\text{Pb}_{0.4}\text{Sr}_2\text{Co}_{1.8}\text{O}_x$ textured ceramics. a) transversal fractured surface, and b) longitudinal polished surface. Different contrasts correspond to $\text{Bi}_{1.7}\text{Pb}_{0.4}\text{Sr}_2\text{Co}_{1.8}\text{O}_x$ (grey), $\text{Bi}_{0.75}\text{Sr}_{0.25}\text{O}_y$ (white), and $\text{Sr}_4\text{Co}_5\text{O}_z$ (dark grey),.

Fig. 3. Temperature dependence of ρ (\bullet) and S (\blacklozenge) for textured $\text{Bi}_{1.6}\text{Pb}_{0.4}\text{Sr}_2\text{Co}_{1.8}\text{O}_x$ materials.

Fig. 4. Temperature dependence of PF for textured $\text{Bi}_{1.6}\text{Pb}_{0.4}\text{Sr}_2\text{Co}_{1.8}\text{O}_x$ materials.

Figure 1

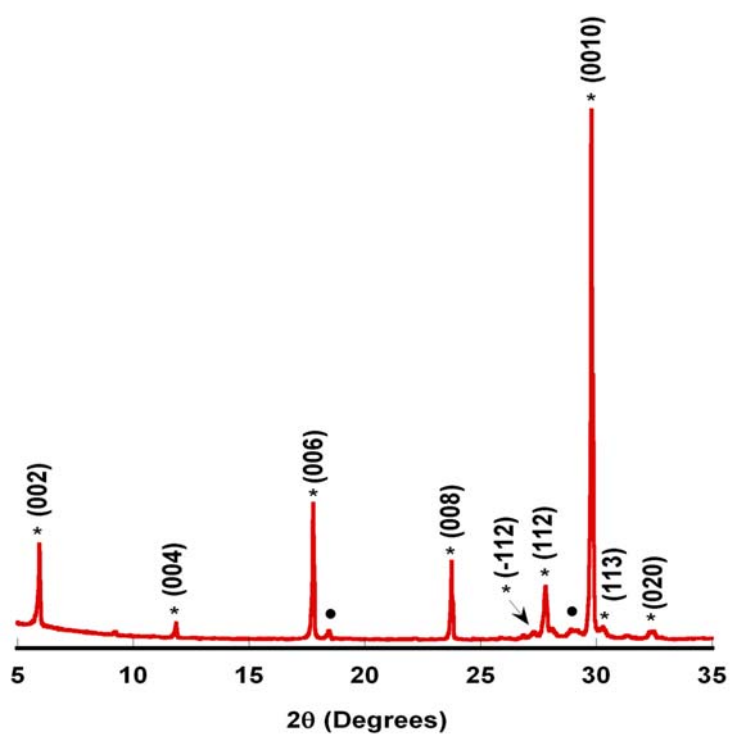


Figure 2

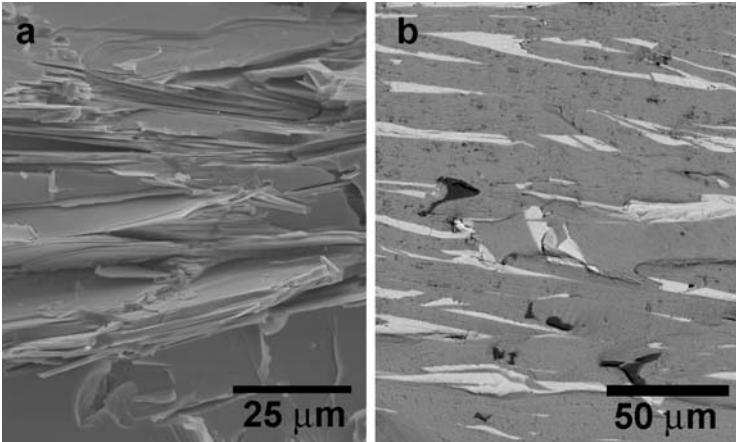


Figure 3

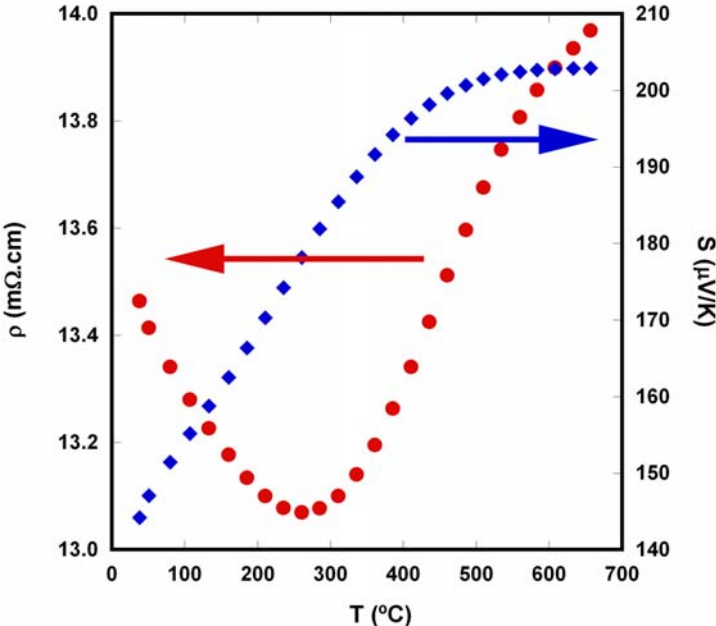


Figure 4

